

## Intercellular calcium waves mediate preferential cell growth toward the wound edge in polarized hepatic cells<sup>☆</sup>

Yen-Jen Sung,<sup>a,c,1</sup> Zulung Sung,<sup>b,1</sup> Chia-Lin Ho,<sup>b</sup> Ming-Te Lin,<sup>a</sup> Jih-Siang Wang,<sup>a</sup> Shun-Chun Yang,<sup>c</sup> Yann-Jang Chen,<sup>d</sup> and Chi-Hung Lin<sup>b,e,\*</sup>

<sup>a</sup> Institute of Anatomy and Cell Biology, National Yang-Ming University, Taipei, Taiwan

<sup>b</sup> Institute of Microbiology and Immunology, National Yang-Ming University, Taipei, Taiwan

<sup>c</sup> Department of Medical Research, Chi-Mei Foundation Hospital, Tainan, Taiwan

<sup>d</sup> Center for General Education, National Yang-Ming University, Taipei, Taiwan

<sup>e</sup> Molecular Cell Biology Center, National Yang-Ming University, Taipei, Taiwan

Received 5 December 2002, revised version received 27 February 2003

### Abstract

During liver regeneration, hepatocytes sense the damage and initiate proliferation of the quiescent cells through poorly understood mechanisms. Here, we have used cultured hepatic cells to study the roles played by intercellular calcium in mediating wound-healing processes. Well-differentiated and polarized Hep-G2 cells repaired an experimentally induced wound by induction of cell divisions. The resulting cellular growth did not occur evenly across the healing cell lawn; instead, proliferations were three times more active within 150–200  $\mu\text{m}$  from the wound edge than further away; this periwound preferential cell growth was not observed in the poorly differentiated and/or nonpolarized cells. We have provided experimental evidence demonstrating that the wounding procedure itself could elicit a propagating calcium wave, and interestingly, blocking this injury-associated intercellular calcium communication could effectively inhibit the biased cell growth along the margin of the wound. A photolithography-based patterned cell culture system was employed to help delineate the mechanisms underlying this type of calcium signaling. In conclusion, our results suggested that intercellular communications via propagating calcium waves coordinate regenerative cell proliferations in response to hepatic tissue losses.

© 2003 Elsevier Science (USA). All rights reserved.

**Keywords:** Wound healing; Proliferation; Calcium wave; Microcontact printing

### Introduction

<sup>1</sup>The wound-healing process is a complex biological activity that has been experimentally investigated in various tissues, including the skin, cornea, gastric mucosa, intestinal epithelium, lung epithelium, retinal pigment epithelial cells, fibroblasts, and endothelium cells, as well as hepatocytes. Studies on wound repair in the liver draw further attention

in that the response of hepatic cells to the injury may be fundamentally similar to liver regeneration [1,2] and the development of hepatic fibrosis (cirrhosis) [1]. Traditionally, the study of liver regeneration is mainly performed on either partially resected (e.g., partial hepatectomy) or drug-treated (e.g., carbon tetrachloride) livers in laboratory animals [1,3,4]. Substantial progress has also been achieved using appropriate transgenic and knockout mouse models for this work [5]. While this approach is powerful for providing crucial in vivo or ex vivo information, the system may be cumbersome for monitoring and analyzing cellular and subcellular events that direct the fine changes and lead to eventual hepatic differentiation and reorganization. In this report, we employed an in vitro hepatic cell model to study the induction of cell proliferations as well as regula-

<sup>☆</sup> Supplemental data associated with this article can be found at doi: 10.1016/S0014-4827(03)00160-5.

\* Corresponding author. Institute of Microbiology and Immunology, National Yang-Ming University, 155, Li-Non St. Sec. 2, Taipei, Taiwan, 112. Fax: +886-2-28212880.

E-mail address: [linch@ym.edu.tw](mailto:linch@ym.edu.tw) (C.H. Lin).

<sup>1</sup> These two authors contributed equally to this study.

tory mechanisms in response to the experimentally induced wound in hepatic cells.

We have previously shown that the hepatoblastoma cell line, Hep-G2, could become differentiated and fully polarized under appropriate culture conditions [6]. When reaching confluence, these cells exhibited a marked reduction of  $\alpha$ -fetoprotein and an increase in albumin secretion [6]. A large number of liver-specific products were also expressed at levels comparable to those found in vivo [7]. Individual cells of the polarized cell monolayer could actively communicate with their neighbors via gap junction [8,9] and by secreted factors [10]. For example, stimulation of connected hepatocytes by glycogenolytic agonists or mechanical injuries have been shown to induce reproducible sequences of intracellular calcium concentration increases, resulting in propagation of intercellular calcium waves in both cultured hepatic cells [11] and the intact liver [12]. Further studies demonstrated that coordination of this type of calcium signaling requires the presence of gap junction permeability that allows the intercellular diffusion of small amounts of inositol 1,4,5-trisphosphate (InsP<sub>3</sub>)<sup>2</sup> [13]. Despite the ample knowledge on the mechanistic nature of calcium oscillations, from which a theoretical model has been built for further experimental tests [14,15], the biological meaning and the downstream effects of hepatic calcium waves remain largely unknown [11,16].

In the present study, we provide evidence demonstrating that mechanical injury-associated intercellular calcium waves might be responsible for triggering cells residing next to the wound to enter cell cycle, resulting in a preferential cell proliferation pattern at the wound margin. This biased growth was only observed in polarized and well-differentiated cells, but not in nonpolarized and/or poorly differentiated cells.

## Materials and methods

### Cell culture

We utilized well-differentiated human hepatoblastoma cell line, Hep-G2 [17], and madin-darby canine kidney (MDCK) epithelial cells [both from American Type Culture Collection (ATCC), Rockville, MD] [18] as polarized cell models. Non-polarized cells used were poorly differentiated human hepatocellular carcinoma cell line, HA22T (a gift from Dr. Cheng-Po Hu at Veterans General Hospital, Taipei, Taiwan) and human cervical carcinoma HeLa cells (ATCC).

### Monolayer wound healing assay

Wounding was typically performed when cultured cells reached confluence and entered a mitotically quiescent

state, following the procedures described by Stolz and Michalopoulos [19] with minor modification. Briefly, confluent monolayers were wounded by scraping the cell lawn with a capillary needle that was installed on a micromanipulator (Narishige MN-188). The scraping force used was such that only minimal scrape depression was rendered on the culture surface, resulting in typical cell-free “wounds” of sizes ranging from less than 50  $\mu\text{m}$  to over 1000  $\mu\text{m}$  depending on the experimental need. Typical healing processes were studied on wounds of 250–500  $\mu\text{m}$  in diameter.

### Quantification of cell proliferation

Incorporation of bromodeoxyuridine (BrdU), a thymidine analogue, was used to detect proliferating cells [20], whereas staining of nuclei with Hoechst 33258 was used to count the cell number in the same microscopic field. BrdU (10  $\mu\text{M}$ ) was added to the culture medium and incubated at 37°C for 20 min. Such BrdU-pulsed cells were fixed with 95% alcohol at room temperature for 20 min, washed twice with a Tris-buffered saline (TBS; 50 mM Tris, 150 mM NaCl, pH 7.4), permeabilized with 0.1% Triton X-100 for 30 min, postfixed with acid alcohol at –20°C for 10 min, then washed with TBS and H<sub>2</sub>O. Nuclear DNA was denatured with 4 N HCl for 15 min, washed twice with H<sub>2</sub>O and once with 0.1 M boric acid solution (pH 8.0), followed by immunostaining with FTIC-labeled antibody against BrdU and nuclear staining with Hoechst 33258. A high-resolution cooled CCD was used for imaging. The MetaMorph program (Universal Imaging Corporation, West Chester, PA) was installed as a central controller for digital imaging acquisition, real-time processing, time-lapse recording, calcium imaging, and subsequent data analysis [6]. Cell proliferation was expressed as proliferation index, where

$$\begin{aligned} \text{proliferation index} \\ &= \frac{\text{number of BrdU-positive cells}}{\text{number of total cells}} \times 100\%. \end{aligned}$$

### Calcium imaging

Calcium Green – 1 AM (Molecular Probes, Eugene, Oregon) was added to live cells at a final concentration of 5  $\mu\text{M}$  and incubated for 30 min at 37°C. Real-time fluorescent images were acquired at video rate (33 ms) and analyzed by the MetaFluor program (Universal Imaging Corporation). For in vivo calcium imaging, we applied 100–200  $\mu\text{l}$  of 5  $\mu\text{M}$  Calcium Green-1 AM directly onto the surface of the liver of an anesthetized rat for 10 min. Fluorescence imaging was then performed under a dissecting microscope (Leica MZ12) equipped with 1.6X objective and 10X ocular lens.

<sup>2</sup> Abbreviations used: AGA, 18 $\alpha$ -glycyrrhetic acid; GJIC, gap junction intercellular communication; InsP<sub>3</sub>, inositol 1,4,5-trisphosphate.

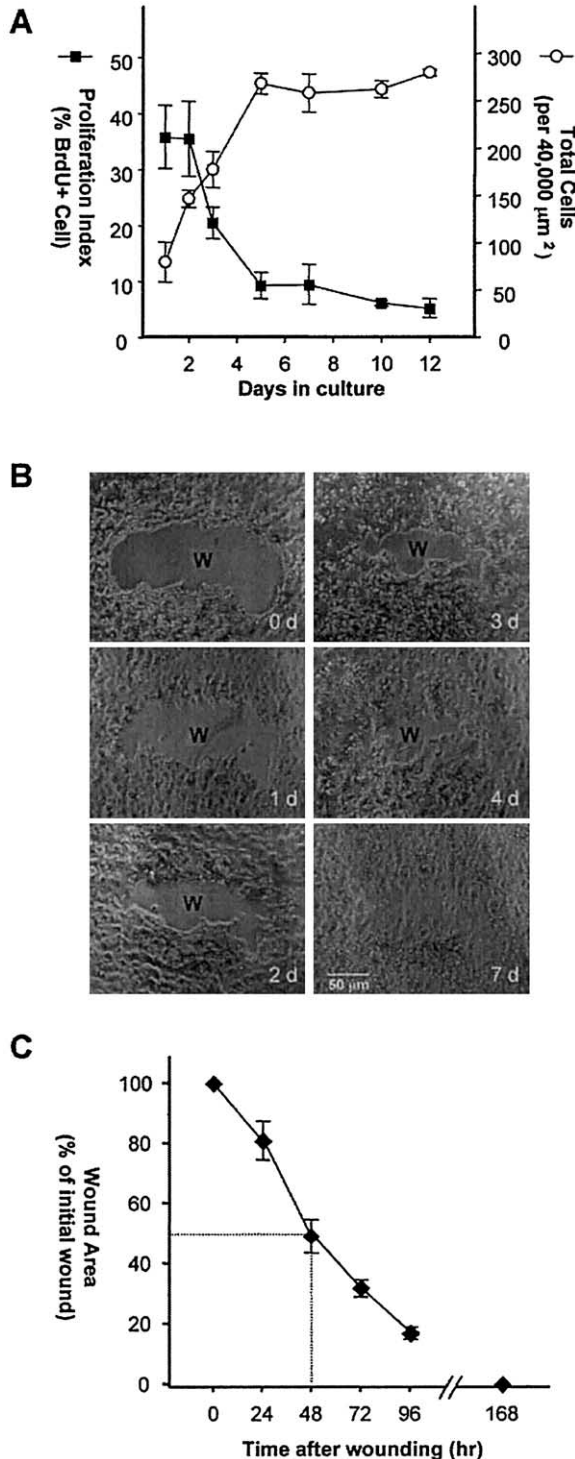


Fig. 1. The wound healing assay. (A) Temporal profile of proliferation and quiescence of Hep-G2 cells under the culture conditions used in this study. Individual cells were visualized by nuclear staining (circles), while cells undergoing proliferation were detected by BrdU incorporation experiments (squares). Note the cells typically reached confluence 5 days after plating (at a cell density of about 270 cells per  $40,000 \mu\text{m}^2$ ), when only  $<10\%$  of cells were BrdU-positive. (B) Sequential images of the wound healing event in Hep-G2 monolayer cells that were well-polarized (5 days after plating). An open wound (W) was created on Hep-G2 monolayer (0 days). During the following 7 days, progressive closure of the wound was observed. Bar,  $50 \mu\text{m}$ . (C) Kinetics of the healing process. The area of the

### Drug treatments

Thapsigargin, BAPTA,  $18\alpha$ -glycyrrhetic acid (AGA), and suramin were all purchased from Sigma. These drugs were first dissolved in DMSO as 1000-fold stock solution before being applied to the cells.

### Microinjection

Microinjection was done using a micropipette (Sutter Instrument) controlled by a micromanipulator. A piezo-driven axial actuator (Burleigh IPZ-100) was used for fine positioning and cell penetration.

### Patterned cell culture

Fabrication of cell growth substrates was done by using microcontact printing [48]. Briefly, silicon masters were first made by standard photolithography procedures using FH-6400L photoresists. The patterned silicon wafer was then passivated by coating with tridecafluoro-1,1,2,2-tetrahydrooctyl-1-triethoxysilane by vacuum deposition. A pre-polymer of polydimethylsiloxane (PDMS) was then cast onto the patterned silicon wafer to make the replica. The resulting PDMS stamp is further treated in oxygen plasma cleaner to render the stamp surfaces hydrophilic. To print proteins, PDMS stamps were inked with laminin solution ( $50 \mu\text{g}/\text{ml}$  in PBS), rinsed briefly with PBS and distilled water, blown dry with a nitrogen gun, then placed in contact with  $2.2 \times 2.2$ -cm glass coverslips.

### Statistics

Quantitative data are presented as the mean  $\pm$  SEM. Statistical analysis was performed using one-way or two-way ANOVA, followed by post hoc Fisher's least significant difference or Dunnett's tests. A  $P < 0.05$  was considered statistically significant.

## Results and discussion

### The wound healing event in mitotically quiescent hepatic monolayer cells

We have investigated the wound healing process in an in vitro human hepatic cell model, a subclone of the Hep-G2 cell line selected for its potent contact inhibition capability. Under our experimental conditions the cultured cells grew

original wound was defined as 100%. While repair was not completed until the seventh day, more than 80% of the healing occurred in the first 96 h. The dotted line indicated 50% healing, which typically occurred at 48 h. Data represent the mean  $\pm$  SEM of five independent experiments in A and C.

actively after plating and typically reached confluence after 5 days (circles, Fig. 1A). Conversely, the percentage of cells undergoing active proliferation (squares, Fig. 1A, as measured by BrdU incorporation experiments) declined from the original  $35.8 \pm 5.5\%$  to a basal level of  $9.4 \pm 2.4\%$  ( $n = 4$ ) after a 5-day culture. To create mechanical wounds on monolayer cell lawns, we scraped capillary glass needles on the quiescent monolayer cells, thereby creating cell free openings with widths ranging from less than  $50 \mu\text{m}$  to over  $1000 \mu\text{m}$  for different experimental requirements. For wounds of  $250\text{--}500 \mu\text{m}$  in diameter (Figs. 1B and C), healing processes typically started at about 12 h after the injury (as wound closure became statistically significant), continued progressively in the following days (especially between 24 and 96 h and reached 50% closure at 48 h, dashed line Fig. 1C), and completed wound repair by 7 days. The hepatic wound repair process observed here was driven mainly by cell proliferation, although cell migration was also involved [1] (data not shown).

#### Cell proliferation of polarized Hep-G2 cell monolayers during the wound healing event

We then examined the extents of cell proliferation during the wound healing event. To identify the actively dividing cells, a short-term (20 min) BrdU labeling procedure was done; these cells were then fixed and stained for the incorporated nucleotide analogues (see Materials and methods). A typical example of this series of experiments is shown in Fig. 2A, where densities of BrdU-positive cells, particularly in the area neighboring the wound margin (dashed lines), were noticed to increase progressively over time. To quantify the mitotic cells surrounding the wound, we calculated the proliferation index within a given periwound segmental area (Fig. 2B) by dividing the numbers of proliferating (BrdU-positive) cells by total (DNA-stained) cells. As shown in Fig. 2C, the proliferation index in the segmental area expanding  $100 \mu\text{m}$  outward from the wound edge significantly increased from  $8.7 \pm 2.6\%$  at 4 h after the wounding to  $36.0 \pm 6.1\%$  measured 48 h later ( $n = 5$ ). We also designed experiments to examine whether such an increase in cell proliferation was indeed induced by mechanical wounding itself or simply by the creation of growth substrate. Monolayer cells were initially grown into confluence in a 0.5-cm-diameter stainless steel cloning ring (C-ring). The ring was then gently lifted, providing these cells a surrounding “cell-free substrate” to grow without mechanical injuries involved. As shown in Fig. 3C, the proliferation index over such C-ring-defined cell lawn was  $17.0 \pm 3.3\%$  (C-ring); cell proliferation in this C-ring-defined cell lawn was significantly less active than that of wound-induced cell growth at 48 h and occurred evenly across the entire cell population without any biased distribution toward the cell lawn border.

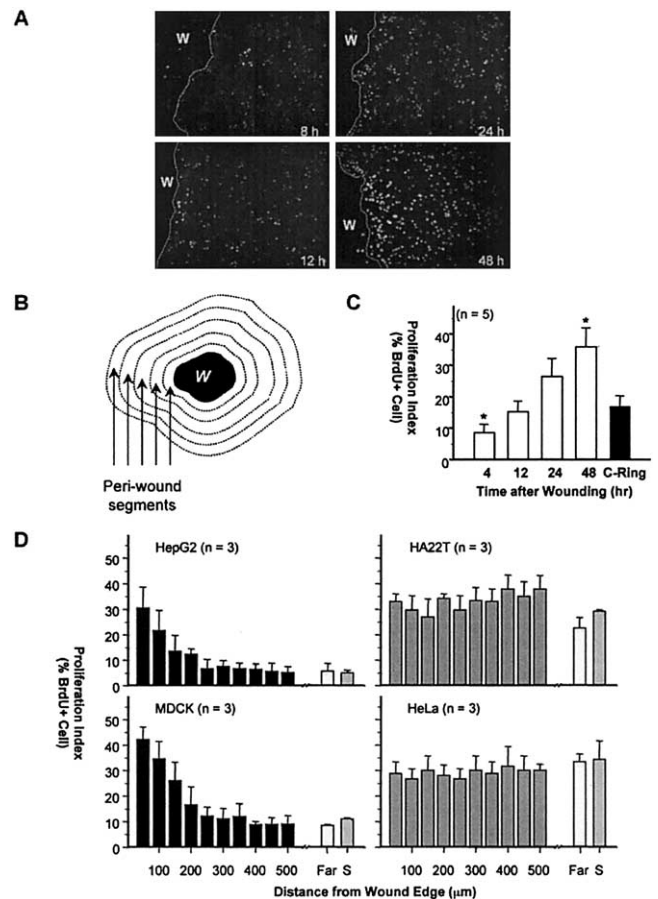


Fig. 2. Biased proliferation pattern following mechanical wounding of polarized Hep-G2 cells. (A) Proliferating cells of the healing cell lawn were detected by BrdU immunofluorescence. Note the BrdU signals increased over time and appeared to accumulate preferentially in cells flanking the wound margin (dashed lines). (B) The quantification scheme of cell proliferation index. Segmental areas of interest (dashed lines) were created by symmetrical expansion of the wounded area (W) at increments of  $50 \mu\text{m}$ . Proliferation index within a certain segmental area was measured by dividing the number of proliferating (BrdU-positive) cells with total cell count. (C) The proliferation index of cells residing within a  $100\text{-}\mu\text{m}$  segmental area was calculated at indicated time points. Note the periwound cell proliferation increased as a function of the healing period, reaching the highest level of  $36.0 \pm 6.1\%$  at 48 h after wounding. In contrast, no such biased cell growth was observed when confluent cell lawns were growing into open culture substrate that was created by lifting the preplanted cloning ring (C-ring). (D) Distributions of BrdU-positive cells in various healing cell models were analyzed when reaching 50% wound closure. The proliferation index within each segmental area was plotted as a function of distance from the wound margin, using cells more than  $5000 \mu\text{m}$  away from the wound (Far, open bars) and on shank wounding plates (S, hatched bars) as controls. Results shown are generated from two well-polarized cell lines, Hep-G2 and MDCK (closed bars), and two nonpolarized cell lines, HA22T/VGH and HeLa (gray bars). Data are means  $\pm$  SEM of 3–5 independent experiments in C and D.

#### Preferential cell proliferation along the wound margin

In the mechanically injured plate, the replicating cells appeared to accumulate preferentially along the wound edge (Fig. 2A). Using the quantification scheme shown in Fig.

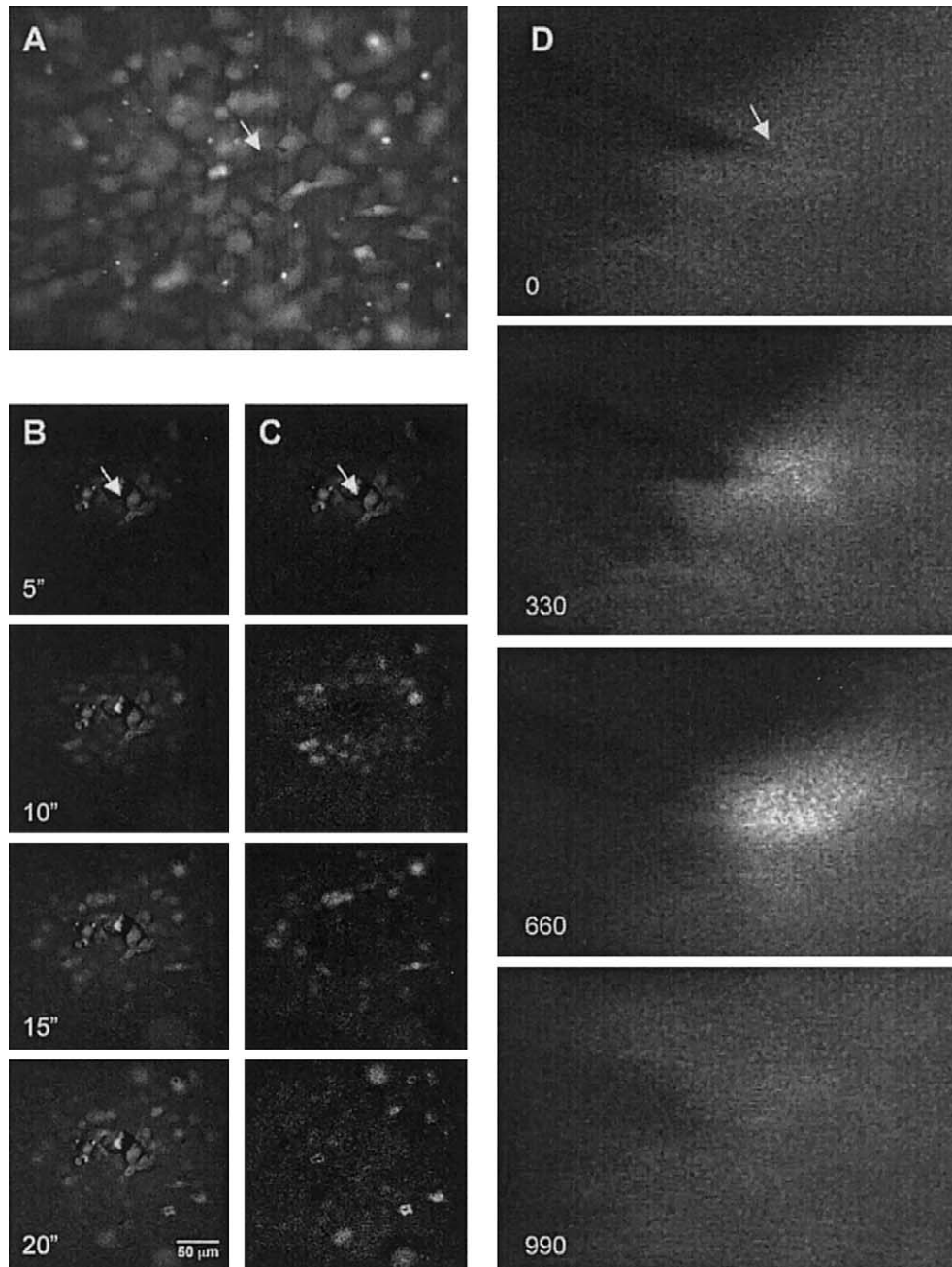


Fig. 3. Propagation of calcium wave induced by mechanical wounding in cultured cells and in the liver of an intact animal. (A) A confluent Hep-G2 monolayer was loaded with an intracellular calcium indicator (Calcium-Green) and injured by microneedle (arrow). (B and C) Fluorescence calcium imaging was performed before and after the trauma. To facilitate the visualization of calcium wave propagation, background subtraction was done at each fluorescent image using 0" frame (B) or the previous frame recorded 5 s earlier (C) as the reference frame. Bar, 50  $\mu\text{m}$  (see supplemental data, wave.mov). (D) The liver of an anesthetized SD rat was exposed, loaded with the cell-permeable calcium dye, wounded by a capillary glass needle (arrow), and observed under a dissecting microscope equipped with a fluorescence module. Immediately after the needle penetration, a transient increase in intracellular calcium concentration occurred at the injured site, propagated outward (0–660), and then subsided (660–990). Time after wounding is shown in milliseconds (see supplemental data, liver.mov).

2B, we further analyzed the cell proliferation indexes as a function of distances from the edge of the wound in a variety of cell lineages when they reached 50% healing; cells located more than 5000  $\mu\text{m}$  away from the wound (open bars), or on the shank operation plates (hatched bars) were used as controls. As shown in Fig. 2D, a preferential

cell growth was noticed in polarized Hep-G2 or MDCK cells within regions about 200  $\mu\text{m}$  from the wound (closed bars); cells further away demonstrated degrees of proliferation comparable with the control conditions. In contrast, the two nonpolarized cell lines tested, HA22T hepatocellular carcinoma cells and HeLa cervical epithe-

lial cells, did not display such a biased pattern of cell growth in response to mechanical wounding (gray bars). The overall levels of BrdU incorporation in these non-polarized cells were higher than those typically associated with the polarized Hep-G2 and MDCK cells and the BrdU-positive cells distributed homogeneously across the entire cell population.

#### *Calcium wave propagation induced by wounding procedure in vitro and in vivo*

The biased pattern of cell proliferation observed in this study raised the question as to whether and what intercellular mechanisms accounted for the delivery of wounding signals. It has been shown that active intercellular communication could be induced by mechanical wounding of the monolayer cells [21] through, for example, calcium wave propagation [12,22]. To address the role of calcium signaling events in hepatic wounding and healing processes, we first examined calcium wave propagation triggered by the injury in polarized Hep-G2 and in the liver of an animal. These experiments are exemplified by the results shown in Fig. 3. Confluent Hep-G2 cells loaded with the calcium indicator, Calcium Green-1 AM, were subjected to glass needle wounding (arrow, Fig. 3A). The traumatic procedure caused a calcium wave that initiated from the injured cells, then propagated outward across neighboring cells at an averaged rate of  $9.6 \pm 0.8 \mu\text{m/s}$  (Figs. 3B and C), traveling an averaged distance of  $193.0 \pm 15.3 \mu\text{m}$  within the first 20 s after the injury. These rates were comparable with previous reports using chemical reagents to induce hepatic calcium waves in hepatocytes [11–13]. Similar results were noticed in polarized MDCK cells (data not shown).

Wounding-induced calcium wave propagation was also observed in intact animals. A typical example is shown in Fig. 3D. Note that penetrating the liver tissue with a microneedle (arrow) immediately elicited a calcium increase transient to that initiated from the injured site, spread outward into the adjacent tissue, then subsided.

#### *Intercellular calcium wave propagation was mediated by both gap junction communication and release of soluble factors*

We then studied the mechanisms underlying the observed trauma-induced calcium signaling events. Pretreatment of the cell lawn with thapsigargin (100 nM), an inhibitor of intracellular calcium store, completely abolished the propagating calcium wave induced by the injury (Fig. 4B). On the other hand, replacing the extracellular medium with a calcium-free solution supplemented with 2 mM EGTA had only minimal effects on the spreading of calcium waves (data not shown), suggesting that the intracellular calcium transient following mechanical trauma was mainly from the release of internal calcium store.

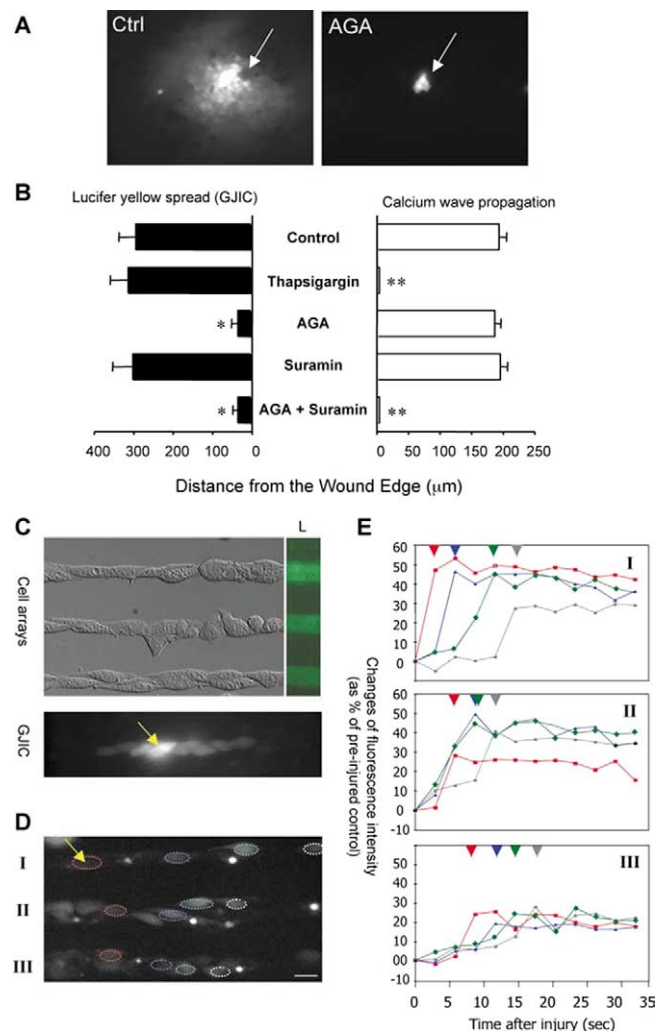


Fig. 4. Mechanistic studies of injury-associated intercellular calcium wave propagation in polarized hepatic cells. (A) The gap junction intercellular communication (GJIC) in polarized Hep-G2 cells was severely interfered with by AGA treatments. Note the microinjected Lucifer yellow was restricted to 1 or 2 cells neighboring the injected cell (arrows), as compared to the spreading over >15 cell diameters typically observed in the mock-treated cells (Ctrl). Bar, 50  $\mu\text{m}$ . (B) The spreading of microinjected fluorescent dye (closed bars), indicative of the integrity of GJIC, and the extent of calcium wave propagation (open bars) from the wound were modulated by various pharmacological reagents. While the addition of AGA could block GJIC (asterisks), only thapsigargin and the combined treatment by AGA and suramin could significantly inhibit calcium wave propagation (\*\* $P < 0.05$ , one-way ANOVA and Dunnett's test). (C–E) Calcium wave kinetics were measured by patterned cell cultures in more details. Characteristic Hep-G2 cell arrays were grown on linear laminin paths (L, visualized by immunofluorescence staining), with intact GJIC as evidenced by dispersion of the fluorescent dye from the injected cell (arrow, C). Calcium imaging was performed in three independent (non-contact) cell arrays (I, II, III, D and E) following the mechanical injury on one cell of cell array 1 (arrow). The changes of fluorescence intensity (as percentage of preinjured control) in representative cells along the cell arrays (individually color-coded in D and E) were plotted as a function of time after the injury. The initiations of calcium transients in these selected cells are indicated (arrowhead in E). Bar, 10  $\mu\text{m}$ .

With regard to the intercellular calcium communication, it has been demonstrated that the calcium wave across cell–cell boundaries could be mediated by either transmis-

sion of small molecules, such as cyclic ADP-ribose and  $\text{InsP}_3$ , via gap junction [23–25], or by release of molecules from injured cells that, in turn, induced calcium transient in the neighboring cells [26,27]. We utilized a combination of pharmacological approaches (Figs. 4A and B) and patterned cell culture system (Figs. 4C–E) to examine these two possible mechanisms.

The integrity of gap junction intercellular communication (GJIC) was assessed by the Lucifer yellow-microinjection assay. As shown in Fig. 4A, the intracellularly introduced small fluorescent dyes were able to cross cell–cell boundaries (through gap junctions), reaching cells  $>250 \mu\text{m}$  (about 10-cell diameters) away from the injected cell. Treating Hep-G2 cells with  $10 \mu\text{M}$  AGA, a gap junctional communication inhibitor [28], could effectively inhibit GJIC; dye spreading was limited to the injected cell itself or cells immediately adjacent to it.

To test the effect of released factors (such as ATP) [29,30] on calcium wave propagation, Hep-G2 monolayers were treated with suramin, a broad-spectrum membrane receptor inhibitor that blocked ATP receptor and its downstream signal transduction pathway [31,32]. As shown in Fig. 4B, addition of either AGA or suramin alone had little effect on trauma-induced calcium wave propagation; combined use of both drugs, on the other hand, could effectively inhibit this form of intercellular communication, suggesting that GJIC and secretory factors both played essential roles in mediating this calcium signaling event.

In addition to these pharmacological studies, we also utilized patterned hepatic cell cultures to further analyze the kinetics of intercellular calcium wave propagation. As shown in Fig. 4C, linear cell arrays could be grown along patterned laminin paths (L) with intact GJIC as evidenced by the spread of injected dye. When a mechanical injury (arrow) was applied to one cell of such a cell array (Figs. 4D and E), we observed not only characteristic calcium wave spreading down the length of this wounded cell array (I) at an average rate of  $7.15 \pm 2.48 \mu\text{m/s}$  ( $n = 16$ , from two independent experiments), but also similar calcium wave propagations along neighboring arrays (II, III) that had no physical contact with the wounded array, suggesting that this form of intercellular communication was likely mediated by soluble factors triggered by the injured cell. The rate of this mode of communication averaged  $5.96 \pm 2.61 \mu\text{m/s}$  ( $n = 46$ , from four independent experiments), comparable to the calculated correlation time  $43.14 \mu\text{m/s}$  [33] according to the experimental condition used in this study.

#### *Preferential cell proliferation along the wound edge was mediated by calcium signaling*

We then examined whether the intercellular calcium wave was indeed involved in modulating or coordinating the proliferative response of monolayer Hep-G2 cells surrounding the wound. The experimental scheme is illustrated in Fig. 5A. Hep-G2 cells were pretreated with various cal-

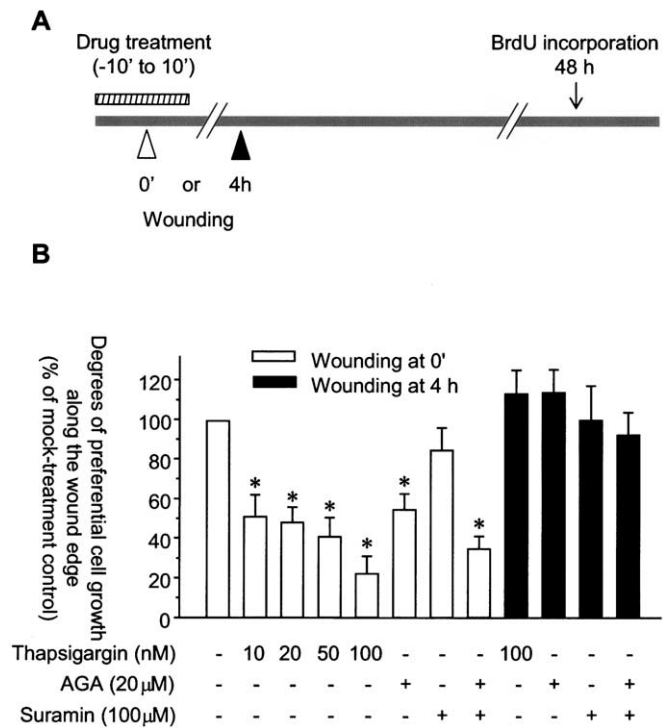


Fig. 5. Perturbation of intercellular calcium wave propagation during the wounding procedure affected the periwound cell proliferation measured 48 h later. (A) The experimental design. Confluent Hep-G2 cells were pretreated with drugs for 10 min, subjected to wounding procedures (open arrowhead), then exposed to the same drugs for another 10 min (hatched bar). After incubation for an additional 48 h, cell proliferation indices were measured by the BrdU incorporation assay (arrow). In control experiments, wounding was performed 4 h after washout of the drugs (solid arrowhead). (B) Wounding was performed in the presence (open bars) or after washout (closed bars) of the chemicals that affected injury-associated calcium wave. Proliferation indexes were measured along the  $100\text{-}\mu\text{m}$  segmental areas surrounding the wound after 48 h healing periods, and normalized by the measurements obtained in the control (vehicle-only) condition. Note that thapsigargin, an effective calcium wave blocker, could inhibit the periwound preferential growth in a dose-dependent manner. While addition of suramin or AGA alone had either little or minor effects, combined use of both drugs was noticed to significantly decrease the preferential cell proliferation along the wound edge. In contrast, wounding cells 4 h after washout of the calcium signal modulators (solid arrowhead, A), when the resumption of intercellular calcium wave propagation could be experimentally verified, all elicited robust periwound cell proliferation (closed bars).  $*P < 0.05$  as compared with the mock treatment control.

cium wave modifiers for 10 min, wounded with a micropipette in the presence of the drugs (open arrowhead), and remained in the same drugs for another 10 min (hatched bar). In the control experiments, wounding was performed 4 h after washout of the pretreatment drugs (closed arrowhead), when the recurrence of the propagating calcium wave could be experimentally verified (data not shown). Proliferation indices of the healing cell lawn along the wound edge were measured 48 h later (arrow).

The results were shown in Fig. 5B. A brief thapsigargin treatment was sufficient to decrease the preferential cell growth along the wound margin in a dose-dependent manner (open bars). At a concentration of  $100 \text{ nM}$  thapsigargin

that completely inhibited calcium wave propagation, there was essentially no preferential growth observed. Similar to the effects on calcium wave propagation, treatments of AGA or suramin alone could only partially inhibit the biased proliferation. However, combined use of both drugs, which completely inhibited the trauma-induced calcium wave propagation as demonstrated in Fig. 4B, had an additive effect in abolishing the biased cell replication along the wound. In control experiments, where wounding was performed after the washout of the calcium wave modifiers, cell growth remained biased along the wound edge (closed bars), suggesting that the observed inhibition of cellular replication in the experimental group was indeed specific to the drug actions.

The very brief drug exposure did not seem to have any long-term adverse effect on cells. The transient drug treatments did not disturb cell cycle progression measured 24 h after washout of the drug (data not shown), and all the drug treatments employed were reversible. Less than 4 h after the drug removal, we were able to elicit full extent of calcium wave propagation (data not shown), suggesting that except for the first 2–3 h, through the entire 48-h experimental period, the healing cells were fully responsive to calcium and calcium-related signaling.

A typical wound-healing process comprises an ordered sequence of events including massive cell migration, proliferation, phenotypic differentiation, and enhanced biosynthetic activities. Resurfacing of the wound is initially accomplished by rapid migration of the cell adjacent to the wound to cover the defect, followed by a later increase in cellular proliferation to restore the cell loss. The migratory activity of the healing hepatic cells is very similar to other types of epithelium (data not shown); however, the induction and/or modulation of cellular proliferation are markedly different comparing polarized to nonpolarized cells.

In the two well-polarized cell lines examined, Hep-G2 and MDCK, the overall extent of cell proliferation during wound repair was less than that of nonpolarized cells (Fig. 2D) or than when these cell were prevented from polarization (data not shown). The less replication may be accounted for by the need of these polarized cells to become “dedifferentiated” before entering the cell cycle. Interestingly, however, the distributions of the replicating cells were not homogenous across the entire healing cell lawn, as was found in the nonpolarized entities; instead, more mitotic cells were found preferentially accumulated near the wound margin (Fig. 2). It appears, therefore, that the wound-neighboring cells were somehow triggered for proliferation by the mechanical wounding employed. The triggering was not from the lack of contact inhibition due to the wound defect, because removal of the cell growth boundary without injuring the cells did not induce the biased cell proliferation (C-ring, Fig. 2C). Our data support the notion that the wounding procedure itself is responsible for the induction of cell replication.

What then is the nature of this induction? How can

traumatic injury to one cell affect its neighbors? The mechanical injury could elicit a propagating intercellular calcium wave as evidenced by our calcium imaging sequence taken *in vitro* (Figs. 2A–C) and *in vivo* (Fig. 2D). Both paracrine [1,34] and GJIC [21,35] seemed to participate in mediating this activity (Fig. 4). To measure these two parameters in a more precise way, we have employed micro-contact printing (Figs. 4C–E) to complement the conventional monolayer cell models. Our results clearly indicated that there were indeed soluble factors participating in the induction of intercellular calcium waves. More studies are being done to further address the molecular mechanisms involved (Ho et al., manuscript in preparation).

Two pieces of our experimental evidence suggested that the induction of cell mitosis at the wound edge is likely mediated by the propagating intercellular calcium wave. First, the biased cell growth seemed to reach the cells 200  $\mu\text{m}$  from the wound edge, a distance comparable to the traveling boundary of the wound-induced calcium wave. The pharmacological treatments that perturbed the calcium transient affected the cell proliferation as well seemingly in a dose–response manner (Fig. 5).

Calcium is at the heart of cell proliferation, differentiation, and even carcinogenesis. It figures prominently in activating proliferatively quiescent normal cells and then triggering chromosome replication and mitosis. Calcium regulates intercellular communication through gap junctions and is also the killer in the programmed suicide mechanism (apoptosis). The wound-induced calcium wave, however, did not seem to influence the degrees of cell death during the repair process (data not shown), another important fine-tuner for the regenerative responses [36].

The trauma-induced calcium wave is not unique to the polarized liver cells. This kind of intercellular communication has been noted in many cultured monolayer cells so long as GJIC was present [37,38]. We did observe propagating calcium waves in the nonpolarized hepatic monolayer cells following wounding; however, calcium influx from outside the cell seemed to account for the major calcium rise observed (data not shown) whereas calcium release from internal stores was predominant when the liver cells became polarized. Indeed, the calcium signaling machinery is subjected to many folds of regulations during hepatic development, differentiation, and regeneration. For example, the phenylephrine-evoked calcium responses are different between differentiated and undifferentiated hepatic doublets [13]. After hepatectomy, the expression of the  $\text{InP}_3\text{R}$ , a key component for relaying the calcium wave, also changed to adapt the calcium signals to the regenerative state [39]. Recent data suggest that regucalcin is responsible for transducing the calcium signaling from the cytoplasm to nuclei in the proliferative cells of regenerating rat liver [40,41]. It is therefore not surprising that although the wound-induced calcium wave was not unique to polarized hepatic cells, a very specific cellular event (i.e., entrance of the cell cycle) could only be elicited in the polarized liver

cells. In support of our findings, perturbations of InsP<sub>3</sub>-based calcium machinery [42] or calmodulin-related signal transduction [43] have both been shown to impair liver regeneration.

Our results highlight the importance of intercellular communication in executing complex cellular events that require coordination of many different types of cells [44], such as the wound healing process. Besides triggering cellular replication at the right time and on the right site as illustrated in this report, GJIC may participate in determining the extent of liver damage that modulates the subsequent regenerative response [45]. Communication via gap junctions also modulates bile secretion [8], glycogenic response to insulin in the liver [46], and so on. Moreover, reduction of gap-junction-mediated communication between hepatocytes can not only protect against progression of liver injury, but also isolate neoplastic cells from growth regulation [47]. Further elucidation of the molecular mechanisms underlying the wound-related intercellular communications is therefore crucial not only in the context of understanding the processes of wound healing and regeneration but also in understanding growth and development, as well as tumor invasion and metastasis.

## Acknowledgments

The authors gratefully acknowledge the inspiration and valuable comments of Dr. Ming-Ta Hsu of NYMU and Dr. Chen-Po Hu of Taipei Veterans General Hospital. Fabrication of silicon master was done at National Nano Device Laboratories and Semiconductor Research Center of National Chiao Tung University. Special thanks go to Mr. Weber Chern at Ta-Ding Corp., Taiwan, for his technical assistance. This work was supported by grants from the National Health Research Institute, and the National Science Council, Taiwan, and the Program for Promoting Academic Excellence of University from the Ministry of Education, Taiwan.

## References

- [1] S.L. Friedman, Cytokines and fibrogenesis, *Semin. Liver Dis.* 19 (1999) 129–140.
- [2] H.M. Mehendale, Role of hepatocellular regeneration and hepatobular healing in the final outcome of liver injury. A two-stage model of toxicity, *Biochem. Pharmacol.* 42 (1991) 1155–1162.
- [3] N. Fausto, Liver regeneration, *J. Hepatol.* 32 (2000) 19–31.
- [4] G.K. Michalopoulos, M.C. DeFrances, Liver regeneration, *Science* 276 (1997) 60–66.
- [5] J.A. Bezerra, T.L. Carrick, J.L. Degen, D. Witte, S.J. Degen, Biological effects of targeted inactivation of hepatocyte growth factor-like protein in mice, *J. Clin. Invest.* 101 (1998) 1175–1183.
- [6] W.N. Lian, J.W. Tsai, P.M. Yu, T.W. Wu, S.C. Yang, Y.P. Chau, C.H. Lin, Targeting of aminopeptidase N to bile canaliculi correlates with secretory activities of the developing canalicular domain, *Hepatology* 30 (1999) 748–760.
- [7] J.B. Parent, H.C. Bauer, K. Olden, Three secretory rates in human hepatoma cells, *Biochim. Biophys. Acta* 846 (1985) 44–50.
- [8] M.H. Nathanson, L. Rios-Velez, A.D. Burgstahler, A. Mennone, Communication via gap junctions modulates bile secretion in the isolated perfused rat liver, *Gastroenterology* 116 (1999) 1176–1183.
- [9] H. Niessen, K. Willecke, Strongly decreased gap junctional permeability to inositol 1,4,5-trisphosphate in connexin 32 deficient hepatocytes, *FEBS Lett.* 466 (2000) 112–114.
- [10] S.F. Schlosser, A.D. Burgstahler, M.H. Nathanson, Isolated rat hepatocytes can signal to other hepatocytes and bile duct cells by release of nucleotides, *Proc. Natl. Acad. Sci. USA* 93 (1996) 9948–9953.
- [11] A.P. Thomas, D.C. Renard-Rooney, G. Hajnoczky, L.D. Robb-Gaspers, C. Lin, T.A. Rooney, Subcellular organization of calcium signalling in hepatocytes and the intact liver, *CIBA Found. Symp.* 188 (1995) 18–49.
- [12] M.H. Nathanson, A.D. Burgstahler, A. Mennone, M.B. Fallon, C.B. Gonzalez, J.C. Saez, Ca<sup>2+</sup> waves are organized among hepatocytes in the intact organ, *Am. J. Physiol.* 269 (1995) G167–G171.
- [13] T. Kitamura, S. Watanabe, K. Ikejima, M. Hirose, A. Miyazaki, A. Yumoto, S. Suzuki, T. Yamada, N. Kitami, N. Sato, Different features of Ca<sup>2+</sup> oscillations in differentiated and undifferentiated hepatocyte doublets, *Hepatology* 21 (1995) 1395–1404.
- [14] G. Dupont, T. Tordjmann, C. Clair, S. Swillens, M. Claret, L. Combettes, Mechanism of receptor-oriented intercellular calcium wave propagation in hepatocytes, *FASEB J.* 14 (2000) 279–289.
- [15] T. Hofer, A. Politi, R. Heinrich, Intercellular Ca<sup>2+</sup> wave propagation through gap-junctional Ca<sup>2+</sup> diffusion: a theoretical study, *Biophys. J.* 80 (2001) 75–87.
- [16] J.F. Whitfield, A.L. Boynton, J.P. MacManus, R.H. Rixon, M. Sikorska, B. Tsang, P.R. Walker, S.H. Swierenga, The roles of calcium and cyclic AMP in cell proliferation, *Ann. NY Acad. Sci.* 339 (1980) 216–240.
- [17] M.M. Zegers, K.J. Zaal, D. Hoekstra, Functional involvement of proteins, interacting with sphingolipids, in sphingolipid transport to the canalicular membrane in the human hepatocytic cell line, HepG2?, *Hepatology* 27 (1998) 1089–1097.
- [18] D.R. Sheff, R. Kroschewski, I. Mellman, Actin dependence of polarized receptor recycling in madin-darby canine kidney cell endosomes, *Mol. Biol. Cell* 13 (2002) 262–275.
- [19] D.B. Stolz, G.K. Michalopoulos, Differential modulation of hepatocyte growth factor-stimulated motility by transforming growth factor beta1 on rat liver epithelial cells in vitro, *J. Cell. Physiol.* 175 (1998) 30–40.
- [20] M.R. Jensen, V.M. Factor, S.S. Thorgeirsson, Regulation of cyclin G1 during murine hepatic regeneration following Dipin-induced DNA damage, *Hepatology* 28 (1998) 537–546.
- [21] J.A. Goliger, D.L. Paul, Wounding alters epidermal connexin expression and gap junction-mediated intercellular communication, *Mol. Biol. Cell* 6 (1995) 1491–1501.
- [22] M.M. Sayeed, Signaling mechanisms of altered cellular responses in trauma, burn, and sepsis: role of Ca<sup>2+</sup>, *Arch. Surg.* 135 (2000) 1432–1442.
- [23] C. Giaume, L. Venance, Intercellular calcium signaling and gapjunctional communication in astrocytes, *Glia* 24 (1998) 50–64.
- [24] J. Sneyd, M. Wilkins, A. Strahonja, M.J. Sanderson, Calcium waves and oscillations driven by an intercellular gradient of inositol (1,4,5)-trisphosphate, *Biophys. Chem.* 72 (1998) 101–109.
- [25] G.C. Churchill, C.F. Louis, Roles of Ca<sup>2+</sup>, inositol trisphosphate and cyclic ADP-ribose in mediating intercellular Ca<sup>2+</sup> signaling in sheep lens cells, *J. Cell Sci.* 111 (Pt. 9) (1998) 1217–1225.
- [26] M. Chanson, P.Y. Berclaz, I. Scerri, T. Dudez, K. Wernke-Dollries, L. Pizurki, A. Pavirani, M.A. Fiedler, S. Suter, Regulation of gap junctional communication by a pro-inflammatory cytokine in cystic fibrosis transmembrane conductance regulator-expressing but not cystic fibrosis airway cells, *Am. J. Pathol.* 158 (2001) 1775–1784.
- [27] N. Rouach, C.F. Calvo, J. Glowinski, C. Giaume, Brain macrophages inhibit gap junctional communication and downregulate connexin 43

- expression in cultured astrocytes, *Eur. J. Neurosci.* 15 (2002) 403–407.
- [28] J.S. Davidson, I.M. Baumgarten, Glycyrhethinic acid derivatives: a novel class of inhibitors of gap-junctional intercellular communication. Structure-activity relationships, *J. Pharmacol. Exp. Ther.* 246 (1988) 1104–1107.
- [29] P.B. Guthrie, J. Knappenberger, M. Segal, M.V. Bennett, A.C. Charles, S.B. Kater, ATP released from astrocytes mediates glial calcium waves, *J. Neurosci.* 19 (1999) 520–528.
- [30] E. Scemes, S.O. Suadicani, D.C. Spray, Intercellular communication in spinal cord astrocytes: fine tuning between gap junctions and P2 nucleotide receptors in calcium wave propagation, *J. Neurosci.* 20 (2000) 1435–1445.
- [31] E. Scemes, R. Dermietzel, D.C. Spray, Calcium waves between astrocytes from Cx43 knockout mice, *Glia* 24 (1998) 65–73.
- [32] K. Braet, K. Paemeleire, K. D'Herde, M.J. Sanderson, L. Leybaert, Astrocyte-endothelial cell calcium signals conveyed by two signaling pathways, *Eur. J. Neurosci.* 13 (2001) 79–91.
- [33] H. Huang, M. Liu, X. Mao, ATP complex of A13+ as studied by PFG NMR, *Spectrochim. Acta (Part A)* 54 (1998) 999–1005.
- [34] T.Y. Ma, M. Kikuchi, I.J. Sarfeh, H. Shimada, N.T. Hoa, A.S. Tarnawski, Basic fibroblast growth factor stimulates repair of wounded hepatocyte monolayer: modulatory role of protein kinase A and extracellular matrix, *J. Lab. Clin. Med.* 134 (1999) 363–371.
- [35] K. Endo, S. Watanabe, A. Nagahara, M. Hirose, N. Sato, Restoration of gap junctions in the regenerative process of ethanol-induced gastric mucosal injury, *J. Gastroenterol. Hepatol.* 10 (1995) 589–594.
- [36] G. Fan, B.T. Kren, C.J. Steer, Regulation of apoptosis-associated genes in the regenerating liver, *Sem. Liver Dis.* 18 (1998) 123–140.
- [37] M. Srinivas, R. Rozental, T. Kojima, R. Dermietzel, M. Mehler, D.F. Condorelli, J.A. Kessler, D.C. Spray, Functional properties of channels formed by the neuronal gap junction protein connexin 36, *J. Neurosci.* 19 (1999) 9848–9855.
- [38] B. Teubner, J. Degen, G. Sohl, M. Guldenagel, F.F. Bukauskas, E.B. Trexler, V.K. Verselis, C.I. De Zeeuw, C.G. Lee, C.A. Kozak, E. Petrasch-Parwez, R. Dermietzel, K. Willecke, Functional expression of the murine connexin 36 gene coding for a neuron-specific gap junctional protein, *J. Membr. Biol.* 176 (2000) 249–262.
- [39] F. Magnino, M. St Pierre, M. Luthi, M. Hilly, J.P. Mauger, J.F. Dufour, Expression of intracellular calcium channels and pumps after partial hepatectomy in rat, *Mol. Cell Biol. Res. Commun.* 3 (2000) 374–379.
- [40] M. Yamaguchi, Role of calcium-binding protein regucalcin in regenerating rat liver, *J. Gastroenterol. Hepatol.* 13 (1998) S106–S112.
- [41] M. Yamaguchi, The role of regucalcin in nuclear regulation of regenerating liver, *Biochem. Biophys. Res. Commun.* 276 (2000) 1–6.
- [42] B.H. Zhang, B.P. Hornsfield, G.C. Farrell, Chronic ethanol administration to rats decreases receptor-operated mobilization of intracellular ionic calcium in cultured hepatocytes and inhibits 1,4,5-inositol trisphosphate production: relevance to impaired liver regeneration, *J. Clin. Invest.* 98 (1996) 1237–1244.
- [43] R.W. Alexander, R. Saydjari, D.G. MacLellan, C.M. Townsend, J.C. Thompson, Calmodulin antagonist trifluoperazine inhibits polyamine biosynthesis and liver regeneration, *Br. J. Surg.* 75 (1988) 1160–1162.
- [44] A.M. Simon, D.A. Goodenough, Diverse functions of vertebrate gap junctions, *Trends Cell Biol.* 8 (1998) 477–483.
- [45] H.M. Mehendale, R.A. Roth, A.J. Gandolfi, J.E. Klaunig, J.J. Lemasters, L.R. Curtis, Novel mechanisms in chemically induced hepatotoxicity, *FASEB J.* 8 (1994) 1285–1295.
- [46] M.U. Siddiqui, S. Benatmane, J.L. Zachary, C. Plas, Gap junctional communication and regulation of the glycogenic response to insulin by cell density and glucocorticoids in cultured fetal rat hepatocytes, *Hepatology* 29 (1999) 1147–1155.
- [47] O. Moennikes, A. Buchmann, K. Willecke, O. Traub, M. Schwarz, Hepatocarcinogenesis in female mice with mosaic expression of connexin32, *Hepatology* 32 (2000) 501–506.
- [48] A. Bernard, J.P. Renault, B. Michel, H.R. Bosshard, E. Delamarche, Microcontact printing of proteins, *Adv. Mater.* 12 (2000) 1067–1070.